

The X-ray nuclei of intermediate-redshift radio sources

M.J. Hardcastle¹, D.A. Evans² and J.H. Croston¹

¹ *School of Physics, Astronomy and Mathematics, University of Hertfordshire, College Lane, Hatfield, Hertfordshire AL10 9AB*

² *Harvard-Smithsonian Center for Astrophysics, 60 Garden Street, Cambridge, MA 02138, USA*

18 April 2018

ABSTRACT

We present a *Chandra* and *XMM-Newton* spectral analysis of the nuclei of the radio galaxies and radio-loud quasars from the 3CRR sample in the redshift range $0.1 < z < 0.5$. In the range of radio luminosity sampled by these objects, mostly FRIIs, it has been clear for some time that a population of radio galaxies (‘low-excitation radio galaxies’) cannot easily participate in models that unify narrow-line radio galaxies and broad-line objects. We show that low-excitation and narrow-line radio galaxies have systematically different nuclear X-ray properties: while narrow-line radio galaxies universally show a heavily absorbed nuclear X-ray component, such a heavily absorbed component is rarely found in sources classed as low-excitation objects. Combining our data with the results of our earlier work on the $z < 0.1$ 3CRR sources, we discuss the implications of this result for unified models, for the origins of mid-infrared emission from radio sources, and for the nature of the apparent FRI/FRII dichotomy in the X-ray. The lack of direct evidence for accretion-related X-ray emission in FRII LERGs leads us to argue that there is a strong possibility that some, or most, FRII LERGs accrete in a radiatively inefficient mode. However, our results are also consistent with a model in which the accretion mode is the same for low- and high-excitation FRIIs, with the lower accretion luminosities in FRII LERGs attributed instead to more efficient radio luminosity production in those objects.

Key words: galaxies: active – X-rays: galaxies

1 INTRODUCTION

1.1 Unified models

Radio galaxies and radio-loud quasars found in low-frequency-selected, flux-limited samples such as 3CRR (Laing, Riley & Longair 1983; hereafter LRL) fall into a number of different observational classes based on their radio and optical emission. Fanaroff & Riley (1974) showed that radio morphology can be related to total radio luminosity; the well-known FRI/FRII division is at a 178-MHz luminosity¹ (L_{178}) of approximately $5 \times 10^{24} \text{ W Hz}^{-1} \text{ sr}^{-1}$. Hine & Longair (1979) pointed out another difference between low-power and high-power sources: at high radio luminosities, radio galaxies are more likely to show strong nuclear optical narrow-line emission. Following Laing et al. (1994) we refer to the weak-line objects, Hine & Longair’s class B, as ‘low-excitation’ radio galaxies (LERG), and the strong-line, class A objects as ‘high-excitation’ sources, although there are some technical differences between the definitions which we will discuss later. It is important to note that the low-excitation/high-excitation division does not correspond to the FRI/FRII division, although most FRIIs are low-excitation objects and most high-excitation objects are FRIIs.

Finally, some high-excitation objects show broad optical emission lines in addition to the narrow lines already discussed. For reasons that are mostly historical, such objects are called ‘broad-line radio galaxies’ (BLRG) if the continuum emission from the optical nucleus does not outshine the host galaxy, and ‘radio-loud quasars’ if it does. The lowest-luminosity object in the 3CRR sample classed as a quasar has $L_{178} \sim 3 \times 10^{26} \text{ W Hz}^{-1} \text{ sr}^{-1}$. High-excitation sources without broad emission lines are called narrow-line radio galaxies (NLRG).

Unified models for radio galaxies (e.g. Urry & Padovani 1995) seek to remove some of this observational complexity by proposing that some of the different observational classes are intrinsically the same objects viewed at different angles to the line of sight, with the differences between them produced partly by the effects of beaming and partly (in some cases) by the effects of an obscuring ‘torus’ containing high column densities of gas and dust. In this paper we shall mostly be concerned with powerful objects, and it is now generally accepted that unified models for powerful radio galaxies and radio-loud quasars (e.g. Scheuer 1987; Barthel 1987, 1989) must be true at some level: that is, at least some radio galaxies must be quasars seen at an unfavourable angle, and so must host ‘hidden’ quasar nuclei.

Barthel (1989) examined 3CRR objects with $0.5 < z < 1.0$, and so with $L_{178} \gtrsim 7 \times 10^{26} \text{ W Hz}^{-1} \text{ sr}^{-1}$, and concluded that it was possible that *all* objects classed as radio galaxies could be

¹ Here, and throughout the paper, we use a concordance cosmology with $H_0 = 70 \text{ km s}^{-1} \text{ Mpc}^{-1}$, $\Omega_m = 0.3$ and $\Omega_\Lambda = 0.7$.

quasars viewed at large angles to the line of sight. At lower luminosities, this model has to be modified for two reasons. Firstly, since there are no objects classed as quasars in the 3CRR sample with $z < 0.3$, but many luminous, FRII-type NLRG, the narrow-line objects in 3CRR must be unified with some other class of object. The unification counterparts of low-luminosity FRII NLRG are almost certainly the BLRG (Laing et al. 1994; Hardcastle et al. 1998) although some BLRG at higher luminosities may be objects seen at viewing angles intermediate between quasars and NLRG. Secondly, while there are almost no low-excitation FRII objects at high radio luminosities, they make up a significant fraction of the population of FRIIs in the two decades of radio luminosity between the FRI/FRII boundary and the luminosity cutoff of Barthel (1989). Since the narrow-line region is too large to be obscured, no change of orientation can allow the low-excitation objects to appear as quasars or BLRG, which always show high-excitation narrow lines. Instead, it seems likely that these objects can appear at any angle to the line of sight without changing their optical classification (except at very small angles to the line of sight, where they may appear as FRII-type BL Lac objects; Laing et al. 1994, Jackson & Wall 1999, Hardcastle et al. 2003). This picture is reinforced by studies of the optical continuum from the nuclei of FRIIs (Chiaberge et al. 2002; Varano et al. 2004) which show that LERGs have optical nuclei that lie on the radio-optical correlation established for FRIs, implying that their optical nuclei are largely unobscured and dominated by jet emission: they argue that the lack of emission lines and of accretion-related continuum (as seen in quasars and BLRG) might imply a low radiative accretion efficiency for LERGs and FRIs, a point we return to later in the paper.

Low-excitation radio galaxies have other properties that set them apart from the population participating in the standard unified model: their linear sizes and core prominences are differently distributed (Laing et al. 1994, Hardcastle et al. 1998), their radio jets and hotspots often have distinctive properties (Hardcastle et al. 1998) and they often lie in denser environments as measured in the X-ray (Hardcastle & Worrall 1999) and optical (Hardcastle 2004). Until now, though, it has not been possible to compare their hard X-ray emission with that seen in NLRG, BLRG and quasars with sufficient spatial resolution to make an unambiguous separation between nuclear and extended emission. This comparison is the subject of the present paper.

1.2 X-ray emission from radio sources

All active nuclei with conventional accretion discs are expected to be intrinsically strong X-ray sources. In unified models, the torus is required to obscure the optical and ultraviolet continuum and the broad-line region of a quasar, and this material will also obscure any X-ray emission from close to the accretion disc. The prediction of unified models was therefore that objects unified with quasars (NLRG) should show a component of heavily absorbed nuclear emission, and this was borne out by early studies of individual objects (e.g. Ueno et al. 1994) as well as more detailed studies of large samples with hard X-ray instruments such as *ASCA* and *Beppo-SAX* (e.g. Sambruna, Eracleous and Mushotzky 1999; Grandi, Malaguti & Focchi 2006). The work of Sambruna et al. also hinted that LERG might have lower nuclear X-ray luminosities than NLRG and broad-line objects, although their sample was heterogeneous. In addition, however, work in the soft X-ray, largely with *ROSAT*, showed that radio-loud AGN had a component of nuclear X-ray emission that was *not* heavily obscured even in NLRG, and was well correlated with the nuclear radio ('core') emission (e.g. Wor-

rall & Birkinshaw 1994; Worrall et al. 1994; Edge & Röttgering 1995; Canosa et al. 1999; Trussoni et al. 1999) implying a relationship with the parsec-scale jet. Although this relationship was best studied in nearby, low-power FRI radio sources, where it was possible to use radio, optical and X-ray data to investigate the relationship between FRI sources and BL Lac objects (e.g. Capetti et al. 2000; Hardcastle & Worrall 2000), the radio-X-ray correlation persisted in FRII radio galaxies (e.g. Hardcastle & Worrall 1999), implying that these more powerful sources had similar jet-related nuclear X-ray properties.

Recently studies with *Chandra* and *XMM-Newton* have confirmed this picture. Using (FRII) 3CRR sources in the redshift range $0.5 < z < 1.0$, where the standard unified model works well, Belsole, Worrall & Hardcastle (2006) reproduce with *Chandra* and *XMM* the radio core/soft X-ray correlation found by Hardcastle & Worrall (1999) with *ROSAT*, while also finding that a large fraction of the NLRG in their sample show an additional heavily absorbed component, as the unified model would predict. Low-redshift ($z < 0.1$) 3C and 3CRR sources, largely FRIs, have been studied by several groups (Donato et al. 2004; Evans et al. 2006 (hereafter E06); Balmaverde et al. 2006): all find that essentially all sources show a soft component of nuclear emission whose luminosity correlates with that of the radio core, as seen with *ROSAT*. E06 found that the narrow-line FRIIs in their sample (which included all 3CRR sources with $z < 0.1$) showed an additional heavily absorbed nuclear component, which was accompanied by Fe K α line emission, and which is most likely to originate near the accretion disc. The properties of the narrow-line FRIIs were thus consistent with the expectation from unified models.

However, the various analyses show that *no* FRI radio galaxy in the 3CRR sample shows any evidence for this type of heavily absorbed nuclear component. Indeed, only one FRI radio galaxy, Cen A, is known to have an energetically dominant component with an absorbing column greater than a few $\times 10^{22}$ cm $^{-2}$ (e.g. Evans et al. 2004). This result has several possible interpretations. If FRI nuclei generally show no absorbed nuclear emission, does this mean that the torus is absent, or that a standard Shakura-Sunyaev accretion disc is absent, or simply that both are present but that the accretion-related X-rays are too weak to be seen? The fact that the FRI and FRII sources lie on the same radio core/X-ray correlation, when the unabsorbed components of the FRIIs are considered, strongly argues that we cannot simply infer that the torus is absent in FRIs while the accretion disc is still present: if this were the case, we would expect the FRIs to have an additional component of unabsorbed X-ray emission, and to lie above the correlation, which is not observed. E06 put constraints on the luminosities of any undetected heavily absorbed components in the FRIs, and showed that they are systematically lower than those of FRIIs, even for sources of comparable radio power, which might argue in favour of a true difference between the accretion luminosities (and hence possibly accretion modes) in FRIs and FRIIs, as previously proposed (e.g. Ghisellini & Celotti 2001). We return to this point later in the current paper.

E06 raised the question of whether there exists a population of FRIIs which, like the FRIs, have jet-dominated X-ray emission. An obvious candidate population is the low-excitation radio galaxies, but in the E06 sample there was only one LERG (3C 388) and, although its properties were consistent with having a weak or absent heavily absorbed component, the nuclear X-ray spectrum was of low quality. Thus both the poorly studied nuclear X-ray properties of LERGs, and the possible similarity between LERGs and the FRI sources studied by E06 and others, motivated us to extend the E06

sample to higher redshifts and obtain more X-ray spectra of both LERG and NLRG radio galaxies. The results of this investigation are the subject of the present paper.

1.3 This paper

In this paper we begin by collating the available *Chandra* and *XMM-Newton* data on the 3CRR sources in the redshift range $0.1 < z < 0.5$, thus filling the redshift and luminosity gap between the samples of E06 and Belsole et al. (2006). We then combine the new data with those of E06 and explore the consequences for the position of LERG in unified schemes, and the nature of the accretion flow in LERG and FRIs.

2 DATA AND ANALYSIS

2.1 Sample

There are 50 objects in the 3CRR sample with $0.1 < z < 0.5$. 16 of these have been observed with *Chandra* and 7 with *XMM-Newton*; 3 have been observed with both, giving a total of 20 sources with useful X-ray data. The X-ray observations cover 6/12 of the objects classed as LERG, 7/26 of the NLRG, 3/7 of the BLRG and 5/5 of the quasars in the sample (see below for more information on classifications), and so are heavily biased away from NLRG; *Chandra*, in particular, has only observed 2 NLRG in this redshift range. We took an early decision to omit 3C 48 from our analysis, since it is a compact steep-spectrum source with peculiar morphology and not obviously unified with either FRIs or FRIIs, and since the short *Chandra* observation has been discussed in detail elsewhere (Worrall et al. 2004). The remaining quasars in the sample are all lobe-dominated with FRII radio morphology. We include X-ray data from two additional $z < 0.1$ FRII radio galaxies, 3C 192 and 3C 285, which were not available to E06, and, since E06 did not determine an explicit upper limit on absorbed emission in 3C 388, we re-analyse that as well. The 22 sources included in our analysis are listed in Table 1. Redshifts and emission-line classifications are taken from the 3CRR catalogue (LRL) with updates from the online version².

It is worthwhile to comment explicitly on the emission-line classifications we use in this paper. These are derived from LRL, and subsequent work on the sample, notably some of the work discussed by Laing et al. (1994); thus, at least to some extent, they reflect a *qualitative* assessment of the nature of the emission-line spectrum, comparable to the classes of Hine & Longair (1979). We take ‘weak-lined’ or ‘absorption-only’ sources in LRL to be LERG in the absence of high-quality spectral data such as those of Laing et al. (1994), and ‘strong-lined’ sources to be NLRG. Jackson & Rawlings (1997) give classifications for some, but not all, sources in the 3CRR sample from data available in the literature, using the quantitative classification of Laing et al. (1994), i.e. that equivalent width of the [OIII] line is less than 10 \AA or that the line ratio [OII]/[OIII] > 1 . The Jackson & Rawlings classifications of FRIIs agree in the vast majority of cases with the qualitative 3CRR classifications that we use for sources in our sample and that of E06, though they do not provide complete coverage of FRIIs with $z < 0.5$. The one disagreement is over 3C 438, which is classed by LRL as absorption-line only (following Smith & Spinrad 1980) but which Jackson & Rawlings class as a high-excitation NLRG.

The evidence for detected [OIII] in 3C 438 (Rawlings et al. 1989) is very weak, however, and its flux is certainly low, and so for consistency we retain 3C 438 in the LERG class. The online table³ collated by Willott et al. (1999) disagrees with both Jackson & Rawlings and LRL in classifying 3C 388 as a high-excitation object, it classifies 3C 295 (unclassified by Jackson & Rawlings) as low-excitation, and it puts two of our sample objects (3C 79 and 3C 223) into the class of weak quasars, which is equivalent to our BLRG class, again disagreeing with Jackson & Rawlings’ classification. Their classification of 3C 79 and 3C 223 is based entirely on nuclear infrared emission – they do not suggest that broad emission lines are directly detected – and hence we feel justified in following LRL and Jackson & Rawlings for these objects. Their classification of 3C 388 refers to Rawlings et al. (1989), who in turn refer to Saunders et al. (1989), who report an estimated [OII]/[OIII] > 1 , so 3C 388 is a LERG, as correctly reported by Jackson & Rawlings. The Willott et al. classification of 3C 295, however, is based on the high-quality spectrum of Lawrence et al. (1996), which does show [OII]/[OIII] > 1 . Varano et al. (2004) argue that 3C 295’s optical properties are more consistent with those of NLRG, and suggest that the source may have been misclassified. For consistency with the classification of the other sources we retain 3C 295 in the NLRG class, but we will explicitly note situations where a reclassification would make a difference to our conclusions.

2.2 Chandra analysis

The archive data were uniformly reprocessed from the level 1 events file with CIAO 3.3 and CALDB 3.2. The latest gain files were applied and the 0.5-pixel randomization removed using standard techniques detailed in the CIAO on-line documentation⁴. No time filtering was carried out apart from applying the standard good time intervals, since the object was to study point sources, which should not be significantly affected by high background. All but one of our targets had a clear detected point source coincident with the nucleus of the host galaxy and the radio core. (The exception, 3C 28, is discussed in Appendix A.) For sources that were not piled up, spectra of the X-ray nuclei were extracted in 2.5-pixel circles (1 pixel is 0.492 arcsec) centred on the visible point-like component, with background taken between 2.5 and 4.0 pixels using the *specextract* script, which also builds the appropriate response files. The small extraction region and local background subtraction ensures that extended thermal emission from the host galaxy, group or cluster is largely removed before fitting. Spectra were grouped, typically to 20 counts per bin after background subtraction.

Chandra observations of several of the sources (3C 47, 3C 109, 3C 215, 3C 219, and 3C 303) are affected by photon pileup. We demonstrated this by calculating the 0.5–7 keV count rates from source-centred circles of radius 1.23 arcsec (2.5 pixels). Typical values are in the range 0.35–0.4 counts per frame, for which a pileup fraction 15–20 per cent is predicted by the PIMMS software. We estimated the spatial extent of the pileup by producing images consisting of grade 7 events, which are largely produced by photon pileup. Inspection of the images showed the pileup to be concentrated within the central 1 arcsec. In order to sample spectra free from pileup, we extracted spectra from the wings of the PSF using source-centred annuli of inner radius 1 arcsec (2.0 pixels) and outer radius 2 arcsec (4.1 pixels), with background sampled from

² <http://3crr.dyndns.org/>

³ <http://www-astro.physics.ox.ac.uk/~cjlw/3crr/3crr.html>

⁴ <http://asc.harvard.edu/ciao/>

Table 1. Sources in the sample, radio and optical information, and X-ray observational data. The columns headed $\log_{10}(L_{178})$ and $\log_{10}(L_5)$ give the log to base 10 of the 178-MHz total luminosity and 5-GHz core luminosity, respectively, in units of $\text{W Hz}^{-1} \text{sr}^{-1}$. Radio data are taken from the online 3CRR catalogue. Where three livetimes are quoted, it indicates that *XMM-Newton* data were used: in this case the livetimes are for the MOS1, MOS2 and pn instruments, in that order.

Source	z	178-MHz flux density (Jy)	α	$\log_{10}(L_{178})$ (W Hz^{-1} sr^{-1})	5-GHz core flux (mJy)	$\log_{10}(L_5)$ (W Hz^{-1} sr^{-1})	Emission line type	Galactic N_{H} ($\times 10^{20} \text{cm}^{-2}$)	Observation ID	Livetime (s)
3C 28	0.1952	17.8	1.06	26.19	<0.2	<21.16	LERG	5.14	3233	49720
3C 47	0.425	28.8	0.98	27.17	73.6	24.43	Q	5.71	2129	44527
3C 79	0.2559	33.2	0.92	26.72	10	23.10	NLRG	10.09	0201230201	16651, 16894, 12255
3C 109	0.3056	23.5	0.85	26.73	263	24.68	BLRG	15.61	4005	45713
3C 123	0.2177	206.0	0.70	27.33	100	23.96	LERG	43.00	829	47016
3C 173.1	0.292	16.8	0.88	26.55	7.4	23.09	LERG	5.25	3053	23999
3C 192	0.0598	23.0	0.79	25.19	8	21.71	NLRG	5.06	0203280201	8559, 8582, 6335
3C 200	0.458	12.3	0.84	26.86	35.1	24.17	LERG	3.69	838	14660
3C 215	0.411	12.4	1.06	26.78	16.4	23.75	Q	3.68	3054	33803
3C 219	0.1744	44.9	0.81	26.47	51	23.47	BLRG	10.38	827	18756
3C 223	0.1368	16.0	0.74	25.79	9	22.50	NLRG	1.20	0021740101	25776, 27382, 18376
3C 249.1	0.311	11.7	0.81	26.44	71	24.13	Q	2.89	0153210101	15379, 17399, 12796
3C 284	0.2394	12.3	0.95	26.22	3.2	22.55	NLRG	1.00	0021740201	43063, 43099, 35806
3C 285	0.0794	12.3	0.95	25.18	6	21.84	NLRG	1.37	6911	39624
3C 295	0.4614	91.0	0.63	27.70	3	23.11	NLRG	1.38	2254	90936
3C 303	0.141	12.2	0.76	25.70	150	23.75	BLRG	1.72	1623	14951
3C 346	0.162	11.9	0.52	25.80	220	24.04	NLRG	5.47	3129	44413
3C 351	0.371	14.9	0.73	26.71	6.5	23.25	Q	2.03	2128	50920
3C 388	0.0908	26.8	0.70	25.63	62	22.97	LERG	5.81	5295	30711
3C 401	0.201	22.8	0.71	26.30	32	23.39	LERG	7.42	3083, 4370	47518
3C 436	0.2145	19.4	0.86	26.31	19	23.22	NLRG	8.20	0201230101	26427, 27833, 22190
3C 438	0.290	48.7	0.88	27.00	7.1	23.07	LERG	17.22	3967	47272

surrounding annuli of inner radius 2 arcsec and outer radius 3 arcsec. We corrected the point-like ancillary response files (ARFs) for the energy-dependent missing flux using the ARFCORR software⁵ that calculates the encircled energy fraction in an annular extraction region of a model PSF created using CHART and MARX⁶.

2.3 XMM analysis

The archive *XMM-Newton* data were reduced using the *XMM-Newton* Scientific Analysis Software (SAS) package. The data were filtered for good time intervals using a count-level threshold determined by examining a histogram of the off-source count rate in the energy ranges 10–12 keV (MOS) and 12–14 keV (pn). GTI filtering resulted in a mean reduction in exposure time of ~ 15 per cent, with the worst case (3C249.1) having a reduction of 30 per cent. The data were then filtered using the flag bitmasks 0x766a0600 for MOS and 0xfa000c for pn, which are equivalent to the standard flagset #XMMEA_EM/EP but include out of field-of-view events and exclude bad columns and rows. They were also filtered for the standard selections of patterns ≤ 12 (MOS) and ≤ 4 (pn).

Spectral analysis was performed using scripts based on the SAS *evselect* tool to extract spectra from all three events lists. We used on-axis response files and ancillary response files generated using the SAS tasks *rmfgen* and *arfgen* (with encircled energy corrections included). All *XMM* targets had a detected compact central X-ray component. Core spectra were extracted from circles of radius 35 arcsec, with background spectra extracted from off-source regions on the same CCD chip. As for the *Chandra* data, spectra

were grouped to a minimum of 20 background-subtracted counts per bin prior to spectral fitting.

2.4 Spectral fitting

Spectral fitting was carried out using XSPEC 11 in the energy range 0.4–7.0 keV (for *Chandra* data) or 0.3–8.0 keV (*XMM-Newton*). For consistency, we followed the same fitting procedure for every source. First, a single power law with fixed Galactic absorption was fitted to the data (see Table 1 for the Galactic column densities used, which are largely derived from the COLDEN software). In one or two cases there was a clear requirement for an excess absorption at soft energies, and in this case a free absorbing column, assumed to be at the redshift of the source, was added to the model. For those sources where a second component of X-ray emission was clearly required (seen in large residuals and poor χ^2 values) we then added a second power law with a free, but initially large, absorbing column at the redshift of the source. This gave rise to good fits in almost all the sources where the χ^2 was initially poor, though occasionally it was necessary to fix the index of the unabsorbed power-law to $\Gamma = 2.0$ to get good constraints on its normalization. (The choice of photon index for the frozen power law clearly affects the resultant normalization, but our tests show that the effect is seen at the 10 per cent level at most for plausible values of Γ .) Errors on the parameters were determined using $\Delta\chi^2 = 2.7$ (90 per cent confidence for one interesting parameter) for consistency with E06. If a single power law provided a good fit to the data, we added a heavily absorbed power law with fixed $\Gamma = 1.7$ and an absorbing column $N_{\text{H}} = 10^{23} \text{cm}^{-2}$ at the redshift of the source and re-fitted. The fixed parameters of this component, particularly the absorption column, are consistent with what is found

⁵ <http://agyo.rikkyo.ac.jp/~tsujimoto/arfcorr.html>

⁶ <http://cxc.harvard.edu/chart/>

in sources with detected heavily absorbed components, and were chosen to agree with the choices of E06; we comment later on the consequences of varying them. If the 90 per cent uncertainty on the normalization of this new component was consistent with zero, we treated the upper bound as an upper limit on a heavily absorbed component. If, on the other hand, the fit was improved with a non-zero normalization for this component, we allowed the absorbing column and, if well-constrained, the photon index of the second power law to vary, and treated the resulting model as a detection of a second component. This in practice only happened for two quasars, 3C 47 and 3C 249.1 (see Appendix A), and clearly in these cases the data would be equally well fitted with a broken power-law model, but we retain the results of the fits for consistency. Additional components, such as a Gaussian around rest energies of 6.4 keV or thermal emission, were added if required by the residuals, as discussed in Appendix A.

We emphasise that the resulting fits are not unique. In many cases the soft component of the spectrum, which we fit with an unabsorbed power law, is only present at the level of one or two spectral bins. In these cases an unabsorbed thermal component with suitably chosen temperature and abundance would clearly give just as good a fit. Even where there are many counts in the unabsorbed component, as in some of our *XMM* datasets, a thermal model with a high temperature can often provide just as good a fit. Our motivations for excluding thermal models in these cases are based on physical plausibility rather than directly on the X-ray spectra. Similarly, we cannot exclude a partial covering origin for the unabsorbed component, although of course the covering fraction in this case would have to vary widely from source to source. Similarly, a scattering model cannot be ruled out. Our motivation for using the model we adopt is based on the existing evidence for a jet-related origin for the soft component; we discuss the evidence for the validity of our approach in the next section.

3 RESULTS

Results of the spectral fits for each source are given in Table 2. Individual sources are discussed, and references to previous work given, in Appendix A. Most of the fits resulting from the procedure we describe above have good reduced χ^2 values, suggesting that the models give adequate representations of the data. For the few sources where the fit is less good, we see no evidence in the residuals for any *systematic* deviation from the models, such as might arise from a missing component in the fits that was present in a number of different sources. We therefore feel able to adopt the qualitative and quantitative results of all the fits in the discussion that follows.

Table 2 immediately shows an interesting difference between the FRII LERG and NLRG. Whereas all (8/8) of the NLRG in our new sample show evidence for a heavily absorbed, luminous component in hard X-rays, consistent with what was observed for the low-redshift sample by E06, all but one (6/7) of the LERG show no such component, and the exception (3C 123) may not be a LERG at all (Section A5). One LERG (3C 28) is undetected, one (3C 173.1) is barely detected, and four others (3C 200, 3C 388, 3C 401, 3C 438) are well fitted with power-law models. If 3C 295, which does show evidence for a heavily absorbed nuclear component, were to be reclassified as a LERG (Section 2.1) then the statistics would be 7/7 NLRG and 6/8 LERG behaving as described above, so the trend is still noticeable.

For quantitative analysis, we combine our sample with the 3CRR sources discussed in E06 to give a total sample size of 40

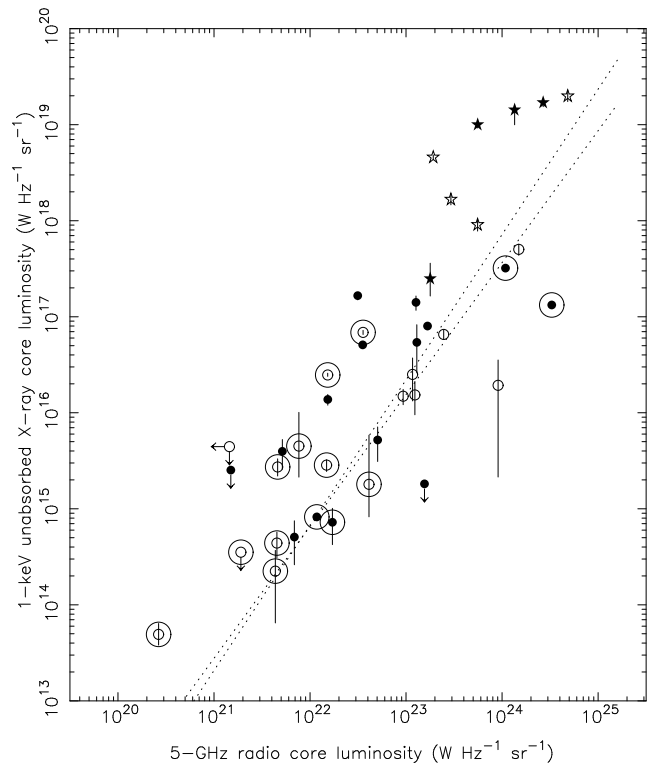


Figure 1. X-ray luminosity of the unabsorbed component for the combined $z < 0.5$ sample as a function of 5-GHz radio core luminosity (Table 1). Open circles are LERG, filled circles NLRG, open stars BLRG, and filled stars quasars. Large surrounding circles indicate that a source is an FRI. Error bars are the 90 per cent confidence limits described in the text. Where error bars are not visible they are smaller than symbols. Dotted lines show the 90 per cent confidence range of regression lines fitted through the NLRGs and LERGs using the maximum-likelihood techniques described by Belsole et al. (2006). BLRGs and quasars lie above this correlation.

X-ray observed objects with $z < 0.5$ (out of 86 in total); this allows comparisons to be made between the LERGs in our sources and the FRIIs in E06. We begin by plotting the 1-keV luminosity of the low-absorption power-law component against the 5-GHz luminosity of the radio core, derived on the assumption of a flat radio spectral index (Fig. 1). This illustrates that the correlation between the soft X-ray emission and the radio core, already discussed by Hardcastle & Worrall (1999), E06 and Belsole et al. (2006), is, unsurprisingly, still present in the $z < 0.5$ sample. As has been found previously (Hardcastle & Worrall 1999) the broad-line objects in the sample lie above the trendline established by NLRG and LERG (which is attributed to the presence of unabsorbed accretion-related emission in the spectra of the BLRG and quasars). However, there is no systematic difference in the behaviour of FRIIs and FRIIs, or NLRG and LERG, although there is a good deal of scatter about the line. Fig. 2 shows the equivalent plot using the total 178-MHz luminosity of the source, illustrating that the correlation is worse when the X-ray luminosities are plotted against an unbeamed quantity; though both are formally well correlated (at > 99.9 per cent significance on a Kendall's T test), the correlation with radio core luminosity is better than with total luminosity, and a partial correlation analysis (partial Kendall's T , neglecting the few upper limits) with redshift as the third variable shows a significant positive partial correlation between the quantities of Fig. 1, but not between those plotted in Fig. 2. The arguments that the correlation between X-ray

Table 2. Results of spectral fitting. For each source the fits, or upper limits, for an absorbed and unabsorbed power law are shown. The model described is the best-fitting model (PL = power law, ABS(PL) = absorbed power law, TH = thermal component, GAU = Gaussian). Components of the fit other than power-law components are discussed in Appendix A. Numerical values marked with a dagger were frozen in the fit (either to derive upper limits or because the data were not good enough to constrain them. 1-keV flux densities and luminosities are the unabsorbed values in all cases.

Source	Net counts	Model	$\chi^2/\text{d.o.f.}$	Component	1-keV flux (nJy)	Photon index	\log_{10} luminosity (ergs s $^{-1}$)	N_{H} ($\times 10^{22}$ cm $^{-2}$)
3C 28	<19	PL	–	PL	<0.5	–	<41.36	–
				ABS(PL)	<3.0	–	<42.27	10.0†
3C 47	1135 \pm 39	PL+ABS(PL)	52.2/44	PL	363 $^{+28}_{-33}$	1.91 $^{+0.24}_{-0.21}$	45.01	–
				ABS(PL)	308 $^{+146}_{-146}$	1.70†	45.05	10.7 $^{+17.6}_{-5.6}$
3C 79	202 \pm 17, 208 \pm 17, 478 \pm 25	PL+ABS(PL)	48.7/44	PL	9.5 $^{+1.6}_{-1.6}$	2.87 $^{+0.31}_{-0.30}$	42.42	–
				ABS(PL)	145 $^{+401}_{-102}$	1.77 $^{+0.69}_{-0.61}$	44.18	24.9 $^{+11.0}_{-8.3}$
3C 109	2611 \pm 57	ABS(PL)	68.2/89	ABS(PL)	896 $^{+129}_{-109}$	1.62 $^{+0.12}_{-0.11}$	45.23	0.5 $^{+0.1}_{-0.1}$
				ABS(PL)	<233.3	–	<44.60	10.0†
3C 123	610 \pm 26	PL + ABS(PL)	21.7/20	PL	1.9 $^{+1.5}_{-1.6}$	2.00†	42.00	–
				ABS(PL)	31.8 $^{+8.3}_{-12.8}$	1.41 $^{+0.49}_{-0.33}$	43.58	3.1 $^{+1.5}_{-1.0}$
3C 173.1	26 \pm 5	PL	–	PL	0.8 $^{+0.3}_{-0.3}$	2.00†	41.55	–
				ABS(PL)	<8.6	–	<43.13	10.0†
3C 192	93 \pm 11, 66 \pm 10, 211 \pm 17	TH+POW+ABS(POW)	21.5/12	PL	5.9 $^{+1.9}_{-2.1}$	1.88 $^{+0.19}_{-0.55}$	41.37	–
				ABS(PL)	159 $^{+87}_{-55}$	1.70†	42.93	51.6 $^{+32.8}_{-16.6}$
3C 200	189 \pm 14	PL	7.3/7	PL	9.1 $^{+1.2}_{-1.2}$	1.72 $^{+0.27}_{-0.25}$	43.58	–
				ABS(PL)	<14.0	–	<43.78	10.0†
3C 215	740 \pm 30	PL	34.6/28	PL	231 $^{+17}_{-17}$	1.80 $^{+0.11}_{-0.11}$	44.84	–
				ABS(PL)	<86.0	–	<44.46	10.0†
3C 219	304 \pm 19	PL	5.6/11	PL	259 $^{+31}_{-31}$	1.90 $^{+0.19}_{-0.18}$	43.99	–
				ABS(PL)	<207.3	–	<44.02	10.0†
3C 223	404 \pm 25, 416 \pm 26, 984 \pm 42	PL+ABS(PL+GAU)	84.7/76	PL	43.5 $^{+3.5}_{-4.2}$	1.62 $^{+0.19}_{-0.21}$	43.16	–
				ABS(PL)	34 $^{+101}_{-15}$	0.71 $^{+0.77}_{-0.61}$	43.67	5.7 $^{+7.8}_{-3.6}$
3C 249.1	9066 \pm 97, 10372 \pm 103, 27819 \pm 170	PL+ABS(PL+GAU)	971.6/970	PL	618 $^{+72}_{-184}$	2.29 $^{+0.30}_{-0.14}$	44.72	–
				ABS(PL)	167 $^{+170}_{-85}$	1.25 $^{+0.25}_{-0.26}$	44.74	0.4 $^{+0.4}_{-0.3}$
3C 284	140 \pm 16, 159 \pm 17, 580 \pm 31	PL+ABS(PL)	51.9/34	PL	4.0 $^{+0.3}_{-0.3}$	2.37 $^{+0.15}_{-0.15}$	42.22	–
				ABS(PL)	98 $^{+340}_{-91}$	1.70†	43.98	161.7 $^{+379.1}_{-47.2}$
3C 285	396 \pm 20	PL+ABS(PL+GAU)	6.4/13	PL	0.4 $^{+0.2}_{-0.2}$	2.00†	40.40	–
				ABS(PL)	227 $^{+60}_{-49}$	1.70†	43.33	32.1 $^{+5.5}_{-4.6}$
3C 295	474 \pm 29	PL+ABS(PL+GAU)	16.8/15	PL	1.0 $^{+0.5}_{-0.5}$	2.00†	42.50	–
				ABS(PL)	82 $^{+172}_{-9}$	1.85 $^{+0.25}_{-0.20}$	44.48	41.0 $^{+7.8}_{-8.4}$
3C 303	245 \pm 18	PL	6.3/9	PL	223 $^{+31}_{-31}$	1.60 $^{+0.21}_{-0.21}$	43.91	–
				ABS(PL)	<227.8	–	<43.86	10.0†
3C 346	3045 \pm 57	PL	99.4/91	PL	58.5 $^{+2.0}_{-2.0}$	1.70 $^{+0.05}_{-0.05}$	43.40	–
				ABS(PL)	<6.4	–	<42.44	10.0†
3C 351	8493 \pm 93	PL+ABS(PL)	235.9/201	PL	7.2 $^{+3.3}_{-2.4}$	5.13 $^{+0.50}_{-0.48}$	41.92	–
				ABS(PL)	167.1 $^{+7.1}_{-11.8}$	1.42 $^{+0.11}_{-0.10}$	44.80	0.8 $^{+0.1}_{-0.1}$
3C 388	183 \pm 16	PL	4.1/5	PL	9.3 $^{+1.7}_{-1.7}$	2.22 $^{+0.30}_{-0.29}$	41.74	–
				ABS(PL)	<8.3	–	<42.01	10.0†
3C 401	406 \pm 29	PL	16.9/16	PL	7.5 $^{+0.8}_{-0.9}$	1.64 $^{+0.21}_{-0.22}$	42.74	–
				ABS(PL)	<16.7	–	<43.05	10.0†
3C 436	192 \pm 17, 183 \pm 17, 564 \pm 29	PL+ABS(POW+GAU)	32.1/35	PL	7.9 $^{+0.6}_{-0.7}$	2.03 $^{+0.24}_{-0.19}$	42.59	–
				ABS(PL)	44 $^{+24}_{-15}$	1.70†	43.53	36.2 $^{+19.9}_{-13.2}$
3C 438	78 \pm 13	PL	1.4/2	PL	1.3 $^{+0.6}_{-0.6}$	1.07 $^{+0.56}_{-0.59}$	42.67	–
				ABS(PL)	<9.2	–	<43.14	10.0†

emission and core radio flux requires that the soft X-ray component of the FRIs and NLRG/LERG FRIs originate in the nuclear jet have been discussed in detail by Hardcastle & Worrall (1999, 2000) and E06, among others, and we will not repeat them here. The key point of relevance to the present paper is that the LERG occupy the same region of parameter space in Fig. 1, and also in other quantities such as the photon index of the fitted power law, as the FRIs and NLRG FRIs. This strongly suggests that the bulk of

the unabsorbed X-ray emission in LERGs (and in the other sources) originates in a jet rather than in an unobscured or partially obscured AGN. Although other models (such as a scattering model) could be devised which might reproduce the X-ray/radio core correlation for a particular class of source, if we accept that the FRI X-ray emission originates in a jet (Section 1.2) then any alternative model requires a coincidence to explain the fact that the *normalizations* of the correlations are indistinguishable in all types of source.

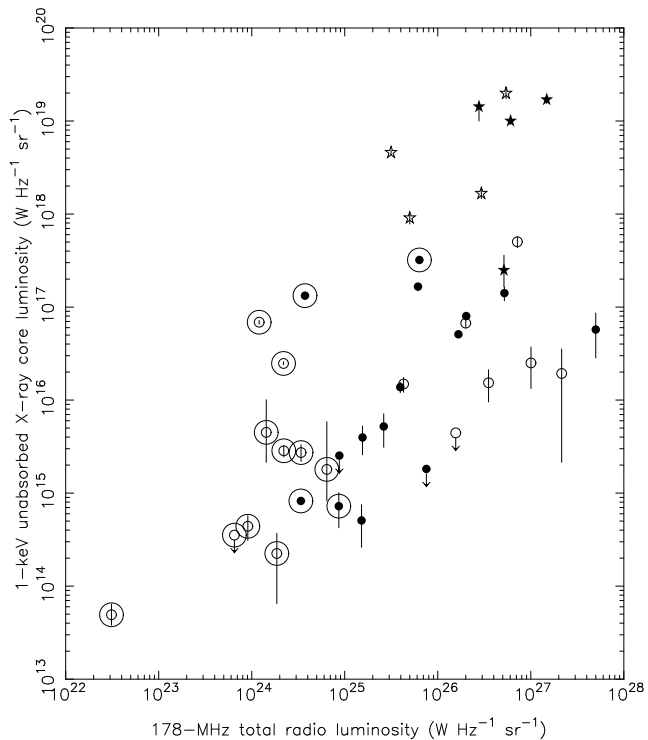


Figure 2. X-ray luminosity of the unabsorbed component for the combined $z < 0.5$ sample as a function of 178-MHz total radio luminosity (Table 1). Symbols as in Fig. 1.

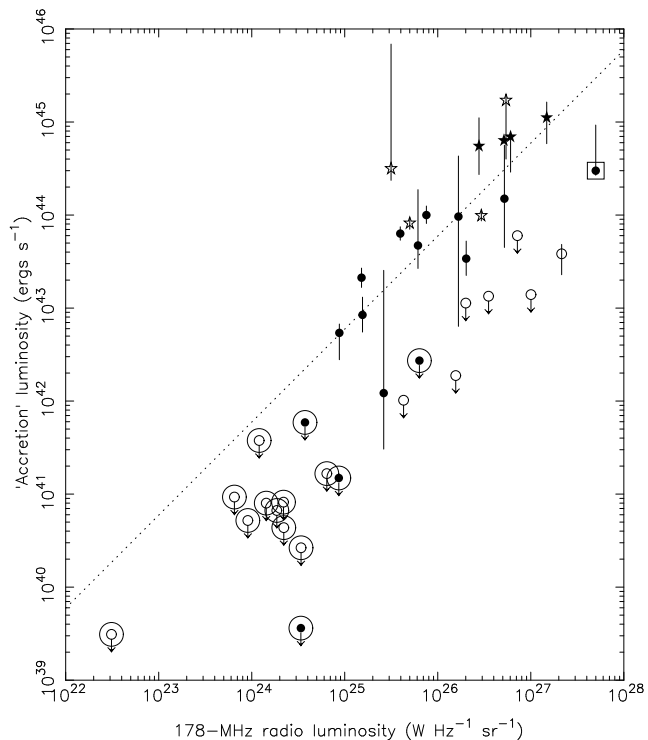


Figure 3. X-ray luminosity of the accretion-related component for the combined $z < 0.5$ sample as a function of 178-MHz total radio luminosity (Table 1). Symbols as in Fig. 1. The dotted line is a line of slope unity whose normalization is determined by the median ratio between the two luminosities for the detected NLRG. A box marks 3C 295, whose status as a NLRG is in doubt.

We now wish to consider the component of X-ray emission that may be related to accretion. The offset of the lobe-dominated quasars and broad-line objects in our sample that are fitted with a single power-law model from the radio core-soft X-ray luminosity relationship (Fig. 1) suggests that in these sources an accretion-related component is dominant; thus, here, the total 2-10 keV luminosity is a reasonable estimate of the accretion-related 2-10 keV luminosity (though ideally we would subtract a contribution from a jet-related component). For the NLRG and the few quasars where a two-component model is a good fit, we can take the accretion-related luminosity to be the unobscured luminosity of the absorbed power-law component: this is supported by the presence of Fe K α emission in a few of the NLRG. In all cases this accretion luminosity is comparable to or larger than (for the NLRG, typically an order of magnitude larger than) the luminosity of the unabsorbed or weakly absorbed component.

Estimating the accretion-related luminosity of the LERGs is harder simply because there is no *a priori* reason to suppose that an obscuring torus exists in these objects (a point we return to later in the paper) so that we do not know whether, or to what extent, any accretion-related luminosity in the LERGs is obscured. However, the 2-10 keV absorption-corrected luminosity we estimate as an upper limit on an obscured component with $N_{\text{H}} = 10^{23} \text{ cm}^{-2}$ is in almost all cases substantially larger than the luminosity of the detected, unobscured component (Table 2). The luminosities could be even larger if the obscuring columns are very much larger in the non-detected objects than in the detected ones: columns of 10^{24} cm^{-2} and higher can increase the ‘hidden’ X-ray luminosities by an order of magnitude or more. As E06 point out, such high column densities and correspondingly high nuclear luminosities are ruled out by infrared data in FRIs (e.g. Müller et al. 2004). The available data are much sparser for LERGs, but we comment on some infrared constraints in Section 4.2. In the meantime, we adopt the limits based on a column density of 10^{23} cm^{-2} , and refer to these, together with the detections for the NLRG, as the ‘accretion-related luminosity’ in what follows; the reader should bear in mind that the upper limits depend on a particular choice of absorbing column, and in particular that they are highly conservative if there is no absorption at all.

A plot of the 2-10 keV accretion-related luminosity against 178-MHz radio luminosity then shows a clear difference between LERGs and NLRGs (Fig. 3). The upper limits on the accretion-related components in the LERGs, given our assumed absorbing column of 10^{23} cm^{-2} , lie systematically below the detected NLRG at all radio powers. In this respect they resemble the FRIs discussed by E06. Both FRIs and FRII LERGs tend to lie below a line of slope unity that passes through the NLRGs. If we interpret the absorbed component in NLRG as directly related to accretion, then this implies that the LERGs and FRIs have lower accretion rates for a given radio luminosity. Only an extreme absorbing column for the LERGs ($> 10^{24} \text{ cm}^{-2}$) could bring them back into agreement with the NLRGs. We discuss the implications of this result in the following section.

4 DISCUSSION

4.1 The nature of LERGs and the FRI/FRII dichotomy

If we neglect for the time being the possibility of an extreme absorbing column in the LERGs, the fact that there is a class of FRII objects (which for convenience we simply refer to as the LERGs

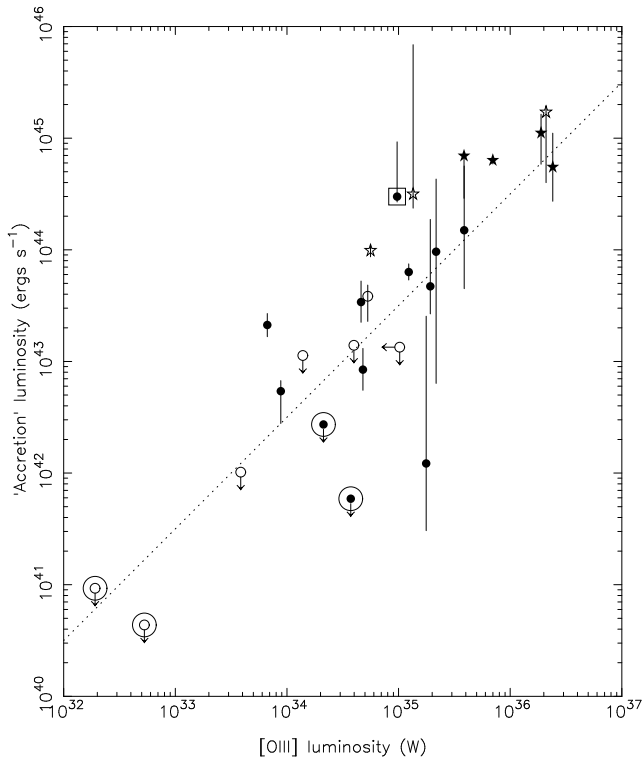


Figure 4. X-ray luminosity of the accretion-related component for the combined $z < 0.5$ sample as a function of power in the [OIII] nuclear emission lines for sources with known [OIII] luminosity. Symbols as in Fig. 1. The dotted line is a line of slope unity with normalization chosen to pass through the NLRG: it is not in any sense a fit to the data. A box marks 3C 295, whose status as a NLRG is in doubt.

in what follows) that have lower accretion power than the NLRGs for a given radio luminosity can be interpreted in two ways. If 178-MHz radio power can be taken to reflect jet power, L_{jet} , then LERGs and NLRGs matched in radio luminosity produce the same L_{jet} for a lower accretion luminosity, L_{acc} ; this could be used, as in model 3 of E06, to argue for a different mode of accretion in the LERGs. If, on the other hand, the observed L_{acc} is an indicator of the true L_{jet} , then LERGs (and FRIIs) manage to produce a greater amount of radio emission for a given L_{jet} ; at a minimum, the LERGs would have to produce about ten times the radio power for a given jet power. The latter model would predict that accretion-related emission might be found at a level predictable from the jet power in LERGs, while in the former model accretion-related emission might not be detected at all.

To distinguish between these models we would need independent measures of the accretion or jet luminosity. One quantity of possible value is the emission-line luminosity. Rawlings & Saunders (1991) have argued that the luminosity in the [OIII] line in FRIIs is well correlated with jet power, and, if it results from photoionization by the nuclear continuum, it should correlate well with accretion power as well. However, Baum, Zirbel & O’Dea (1995) have shown that the slope and normalization of radio luminosity-emission line correlations are different for FRI and FRII populations, and argue that it is possible that the (mostly low-excitation) FRIIs produce emission lines by a different mechanism, which may not be related to the active nucleus at all. We cannot rule out the possibility that this is true for the LERG FRIIs as well (the presence of a LERG population among the FRIIs was not considered

by either Rawlings & Saunders or Baum et al.) and in fact Chiaberge et al. (2002) show that the FRIIs and LERG FRIIs in their sample lie in a regime where it is possible that the [OIII]-emitting regions are photoionized not by an AGN but by the optical (synchrotron) emission from the jet. However, [OIII] luminosities are readily available for FRIIs and a few FRIIs⁷ and we plot accretion-related luminosity against [OIII] luminosity for the objects with available emission-line data in Fig. 4. Although there is clearly significant scatter in this plot (including error bars, the total range in X-ray luminosities for an [OIII] luminosity of 10^{35} W is up to four orders of magnitude) what is interesting about it is that the LERG and NLRG (and the few FRIIs with available data) do appear to lie in positions consistent with a linear relationship between emission-line luminosity and accretion luminosity. Thus we cannot rule out a model in which there are conventional active nuclei, with somewhat lower L_{acc} than would be predicted from their radio luminosity, present in the LERGs and producing both X-ray and optical line emission: and if we were to assume that the Rawlings & Saunders (1991) result holds for LERGs, this result would favour the model in which it is purely the relationship between L_{jet} and 178-MHz radio luminosity that is different about the objects classed as LERGs. This model is also favoured by the existence of up to two LERGs (3C 123 and possibly 3C 295: see Section 2.1) that do show detected heavily absorbed components, albeit as a somewhat low level for their radio luminosity – bearing in mind that neither of these is entirely securely classed as a LERG.

However, it is important to remember that there is no direct evidence for the existence of an obscuring ‘torus’ in FRII LERGs in general, just as there is no such evidence in all but a few FRIIs. If there is no torus, then the upper limits on any accretion-related luminosity in the LERGs would be much lower, and they would no longer lie anywhere near the straight-line relationship of Fig. 4. Thus it is worth considering the consequences of the alternative model, in which the objects that lie below the L_{178} - L_{acc} relationship of Fig. 3, both LERGs and FRIIs, do so as a result of a different accretion mode.

The idea that FRIIs may accrete in an advection-dominated mode, leading to low luminosities from the accretion flow (e.g. Fabian & Rees 1995), has a long history (e.g. Baum, Zirbel & O’Dea 1995; Reynolds et al. 1996; Ghisellini & Celotti 2001; Donato et al. 2004, E06, model 3). The main difficulty from the point of view of radio-galaxy physics with such a model is that the FRI/FRII dichotomy, and its dependence on host galaxy properties (Ledlow & Owen 1996), can be explained purely in terms of jet power and the interaction with the environment (e.g. Bicknell 1995). Indeed, an environmental, rather than nuclear, origin for the FRI/FRII transition seems inescapable given the existence of (rare) sources with hybrid morphologies (Gopal-Krishna & Wita 2000). Moreover, it is well known that the parsec-scale jets of FRIIs and FRIIs are observationally similar, arguing against a difference between the classes of source on this scale (e.g. Pearson 1996; Giovannini et al. 2001). Explaining how a different accretion mode *must* produce a different kpc-scale jet was thus both difficult and, in some sense, unnecessary. If we accept that both FRI

⁷ We use the online table collated by Willott et al. (1999) and previously discussed in Section 2.1, corrected for the cosmology used in this paper. Given the very large scatter in line ratios observed in the Willott et al. compilation, and the fact that LERG and BLRG are expected to differ in [OII]/[OIII] line fluxes, we do not attempt to supplement the true [OIII] fluxes with values estimated from the luminosities in other lines such as [OII].

and FR II kpc-scale structures can be produced by nuclei with low accretion luminosity (similar to the picture presented by Chiaberge et al. 2002 and Marchesini, Celotti & Ferrarese 2004) then this problem is removed. Instead, we can accommodate both FRIIs with low-luminosity accretion flows, like the LERGs, and FRIIs with relatively high-luminosity accretion flows (Cen A being one example, and the FRI quasar of Blundell & Rawlings 2001 another) in a scheme in which environment, L_{jet} and L_{acc} , the last two presumably governed by parameters of the black hole system like \dot{m} , M and spin, all play a role.

If the population of LERGs and FRIIs with low accretion luminosity are identical, how does this fit with the other known distinctive properties of LERGs? Clearly the low-excitation optical nuclei are easily explained: there is no luminous AGN to provide the ionizing continuum necessary for strong optical emission lines (cf. Chiaberge et al. 2002). The situation with respect to their distinctive environments (Section 1.1) is less clear. Of the 7 FR II sources we class as LERGs, the *Chandra* data (and earlier studies, in several cases) show 5 (3C 28, 3C 123, 3C 388, 3C 401, 3C 438) to lie in rich clusters, consistent with the findings of Hardcastle (2004), which were based on the galaxy counts of Harvanek et al. (2001). With the exception of 3C 295, the most luminous NLRG in the sample (whose status as a NLRG is in doubt: see Section 2.1), none of the NLRG FRIIs lies in a gas-rich environment. Thus, it remains possible (and this is true whatever the interpretation of the low accretion luminosities seen in X-ray) that some of the LERGs have intrinsically low-luminosity jets and an artificially high low-frequency radio luminosity as a result of their rich environments and consequent high internal energy densities (cf. Barthel & Arnaud 1996), with other morphological peculiarities (bright jets, weak hotspots, distorted lobes) found in several of these sources being, similarly, a result of the interaction between the jet and the rich cluster environment. It is noteworthy that the objects classified as LERGs that are certainly not in rich environments (3C 173.1 and 3C 200) are entirely morphologically normal FRIIs. It therefore seems plausible that the cluster-centre LERGs form a distinct population whose peculiarities are a result of their environment, and do not need to be explained as a direct result of their nuclear properties. We note that the cluster-centre FRIIs would, in general, be expected to be hosted by especially massive galaxies, with correspondingly large central black holes, and therefore would have a lower value of the fractional accretion rate parameter (\dot{m}/M_{BH} : expected to control the mode of accretion) for a given \dot{m} than NLRG FRIIs in poorer environments. Such cluster-centre objects also have a ready supply of fuel, via Bondi accretion from the dense cluster gas, which is not available to NLRG in poorer environments.

4.2 Implications for unified models of FRIIs

Our results on LERGs reinforce the idea that these objects cannot be unified with BLRG and quasars. A prediction to be made from this is that the objects that *are* FR II LERGs seen at a small angle to the line of sight (these might include BL Lac objects with FR II radio structures) might share some of the peculiar features of the LERG population, such as dense environments. This is in principle testable with X-ray observations of suitable BL Lac objects.

Our results also allow us to comment on the unification of NLRG FRIIs and BLRG/quasars. The universal detection of a heavily absorbed nuclear component in the NLRGs is of course *qualitatively* consistent with the expectation from unified models. Like Belsole et al. (2006) we find that the unabsorbed accretion luminosities of many of the NLRG are similar to the luminosities

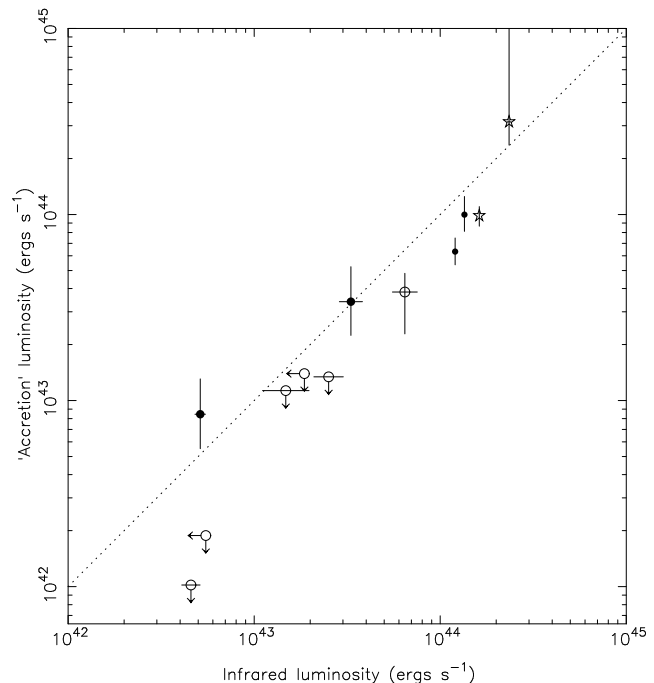


Figure 5. X-ray luminosity of the accretion-related component for the combined $z < 0.5$ sample as a function of luminosity in the mid-infrared (νL_ν at $15 \mu\text{m}$), taken from Ogle et al. (2006), for 12 sources with both infrared and X-ray measurements or upper limits. The dotted line is the line of equality between the two luminosities, and is independent of the data.

of BLRG and quasars in the same range of radio power: this represents a measure of quantitative consistency with unified model predictions. We see (e.g. Fig. 3) that the luminosities of quasars and BLRG tend to lie slightly above those of the NLRG; Belsole et al. attribute the same tendency in their sample to the presence of beamed, jet-related X-ray emission in the BLRG and quasars which has been separated out by differing absorption columns (and would be weaker in any case) in the NLRG. Although the core/soft X-ray correlation (Fig. 1) is not well enough constrained to make a definite statement, estimated corrections to the BLRG/quasar luminosity from subtracting the jet-related component range from 5 to 40 per cent, enough to move many of the broad-line objects significantly lower on Fig. 3. The photon indices of the absorbed components in radio galaxies, where well constrained, occupy the same range as those of the unabsorbed power laws fitted to broad-line objects, which is also consistent with the simple unified model expectation.

A few of the detected NLRG FRIIs in our sample have accretion-related X-ray luminosities $< 10^{43} \text{ ergs s}^{-1}$, significantly below the $\sim 10^{44} \text{ ergs s}^{-1}$ of the least luminous detected BLRG. This is reminiscent of the results of Ogle, Whyson & Antonucci (2006) who have recently used *Spitzer* data to show that some radio galaxies do not have a luminous ($> 10^{44} \text{ ergs s}^{-1}$) mid-infrared nucleus. Some of the ‘mid-infrared weak’ sources of Ogle et al. are objects that we class as LERGs, which we might expect to form a separate population, but others are NLRGs, including two in our sample, 3C 192 and 3C 436. Our X-ray data for these sources allow us to say with certainty that, while they may not host a ‘luminous accretion disc’ by the definition used by Ogle et al., they certainly do host a heavily obscured nuclear component and would appear quite different in the X-ray if the obscuration were removed. Occam’s razor suggests that these NLRG would be expected to have

BLRG counterparts of similar accretion luminosity. Having said this, the correlation between the accretion and mid-IR luminosities for the few sources in common between the sample of Ogle et al. and ours (Fig. 5) is remarkable: the sources that they find to have low infrared luminosity have exactly corresponding low X-ray luminosity. This result provides a foretaste of what may be expected when comparisons of X-ray and infrared data for larger numbers of sources are available, as discussed by Belsole et al.

Finally, we note that the fact that the LERGs in common between the two samples lie near or below the line of equality in Fig. 5 strongly suggests that we have not grossly underestimated the true LERG accretion luminosity, at least in these sources. If the column densities for these objects were $\gtrsim 10^{24} \text{ cm}^{-2}$, the upper limits on the ‘hidden’ nuclear luminosities would be 1 or more orders of magnitude higher than the upper limits we have plotted, and if the true luminosities were close to the upper limits, we should see a correspondingly large nuclear luminosity re-radiated in the infrared, which is not observed. This retrospectively justifies our choice of a limiting column density of 10^{23} cm^{-2} .

5 SUMMARY AND CONCLUSIONS

Our results and conclusions can be summarized as follows.

- While normal NLRG universally show a heavily absorbed component of nuclear X-ray emission, this is rarely found in low-excitation FRIIs (LERGs): thus the LERGs are observationally similar in their properties to the FRIIs studied by E06, mostly showing only unobscured X-ray emission that we attribute to the parsec-scale jet.

- Discounting the possibility of absorbing columns significantly greater than 10^{23} cm^{-2} , we can place upper limits on the luminosity of any undetected accretion-related component present in the LERGs which are substantially below the values for detected NLRG of similar total radio luminosities.

- Some lines of evidence, notably a reasonable correlation between accretion luminosity and [OIII] emission line luminosity that would exist if the accretion luminosities are close to the upper limit values, support the idea that (at least some of) the LERGs do have absorbed nuclear components from a conventional accretion disc, but at a level lower than would be inferred from their radio luminosities. This would imply that the LERGs are of the order of 10 times more efficient than the NLRG at producing low-frequency radio emission for a given accretion luminosity, which may relate to the rich environments of many LERG sources.

- However, there remains a strong possibility that some, or most, FRII LERGs accrete in a radiatively inefficient mode, and have little or no X-ray accretion-related emission, as has been previously argued for FRI sources. Allowing both FRI and FRIIs to be generated by an active nucleus powered by a radiatively inefficient accretion flow removes some of the problems of earlier models along these lines. The FRI/FRII dichotomy in this picture would remain a function of jet power and source environment, while the low-excitation/high-excitation dichotomy would be controlled by the accretion mode and thus presumably by black hole mass and accretion rate. There is no requirement for dusty tori in the LERGs, but we cannot rule out the possibility that they exist.

- Finally, we show that the accretion luminosities of the NLRG and broad-line objects (BLRG and quasars) in our sample are roughly consistent. Some NLRG have low-luminosity absorbed nuclei, but we argue that such objects must still participate in normal unified models.

ACKNOWLEDGEMENTS

MJH thanks the Royal Society for a research fellowship. This work is partly based on observations obtained with *XMM-Newton*, an ESA science mission with instruments and contributions directly funded by ESA Member States and the USA (NASA). We are grateful to Marco Chiaberge and to the anonymous referee for comments that helped us to improve the paper.

REFERENCES

- Allen, S.W., Fabian, A.C., 1992, *MNRAS*, 258, 29P
 Allen, S.W., Fabian, A.C., Idesawa, E., Inoue, H., Kii, T., Otani, C., 1997, *MNRAS*, 286, 765
 Balmaverde, B., Capetti, A., Grandi, P., 2006, *A&A*, 451, 35
 Barthel, P.D., 1987, in Zensus J., Pearson T., eds, *Superluminal Radio Sources*, Cambridge University Press, Cambridge, p. 148
 Barthel, P.D., 1989, *ApJ*, 336, 606
 Barthel, P.D., Arnaud, K.A., 1996, *MNRAS*, 283, L45
 Baum, S.A., Zirbel, E.L., O’Dea, C.P., 1995, *ApJ*, 451, 88
 Belsole, E., Worrall, D.M., Hardcastle, M.J., 2006, *MNRAS*, 336, 339
 Bicknell, G.V., 1995, *ApJS*, 101, 29
 Blundell, K.M., Rawlings, S., 2001, *ApJ*, 562, L5
 Canosa, C.M., Worrall, D.M., Hardcastle, M.J., Birkinshaw, M., 1999, *MNRAS*, 310, 30
 Capetti, A., Trussoni, E., Celotti, A., Feretti, L., Chiaberge, M., 2000, *MNRAS*, 318, 493
 Chiaberge, M., Capetti, A., Celotti, A., 2002, *A&A*, 394, 791
 Comastri, A., Brunetti, G., Dallacasa, D., Bondi, M., Pedani, M., Setti, G., 2003, *MNRAS*, 340, L52
 Croston, J.H., Birkinshaw, M., Hardcastle, M.J., Worrall, D.M., 2004, *MNRAS*, 353, 879
 Donato, D., Sambruna, R.M., Gliozzi, M., 2004, *ApJ*, 617, 915
 Edge, A.C., Röttgering, H., 1995, *MNRAS*, 277, 1580
 Evans, D.A., Kraft, R.P., Worrall, D.M., Hardcastle, M.J., Jones, C., Forman, W.R., Murray, S.S., 2004, *ApJ*, 612, 786
 Evans, D.A., Worrall, D.M., Hardcastle, M.J., Kraft, R.P., Birkinshaw, M., 2006, *ApJ*, 642, 96
 Fabian, A.C., Rees, M.J., 1995, *MNRAS*, 277, L55
 Fanaroff, B.L., Riley, J.M., 1974, *MNRAS*, 167, 31P
 Ghisellini, G., Celotti, A., 2001, *A&A*, 379, L1
 Giovannini, G., Cotton, W.D., Feretti, L., Lara, L., Venturi, T., 2001, *ApJ*, 552, 508
 Gopal-Krishna, Wiita, P., 2000, *A&A*, 363, 507
 Grandi, P., Malaguti, G., Fiocchi, M., 2006, *ApJ*, 642, 113
 Gutierrez, K., Krawczynski, H., 2005, *ApJ*, 619, 161
 Hardcastle, M.J., 2004, *A&A*, 414, 927
 Hardcastle, M.J., Alexander, P., Pooley, G.G., Riley, J.M., 1998, *MNRAS*, 296, 445
 Hardcastle, M.J., Birkinshaw, M., Worrall, D.M., 2001, *MNRAS*, 323, L17
 Hardcastle, M.J., Birkinshaw, M., Cameron, R., Harris, D.E., Looney, L.W., Worrall, D.M., 2002, *ApJ*, 581, 948
 Hardcastle, M.J., Worrall, D.M., 1999, *MNRAS*, 309, 969
 Hardcastle, M.J., Worrall, D.M., 2000, *MNRAS*, 314, 359
 Hardcastle, M.J., Worrall, D.M., Birkinshaw, M., Canosa, C.M., 2003, *MNRAS*, 338, 176
 Harris, D.E., et al., 2000, *ApJ*, 530, L81
 Harvanek, M., Ellingson, E., Stocke, J.T., Rhee, G., 2001, *AJ*, 122, 2874
 Hine, R.G., Longair, M.S., 1979, *MNRAS*, 188, 111
 Jackson, C.A., Wall, J.V., 1999, *MNRAS*, 304, 160
 Jackson, N., Rawlings, S., 1997, *MNRAS*, 286, 241
 Kataoka, J., Edwards, P., Georganopoulos, M., Takahara, F., Wagner, S., 2003, *A&A*, 399, 91
 Laing, R.A., Jenkins, C.R., Wall, J.V., Unger, S.W., 1994, in Bicknell G.V., Dopita M.A., Quinn P.J., eds, *The First Stromlo Symposium: the Physics of Active Galaxies*, ASP Conference Series vol. 54, San Francisco, p. 201

- Laing, R.A., Riley, J.M., Longair, M.S., 1983, MNRAS, 204, 151 [LRL]
 Lawrence, C.R., Zucker, J.R., Readhead, A.C.S., Unwin, S.C., Pearson, T.J.,
 Xu, W., 1996, ApJS, 107, 541
 Lawson, A.J., Turner, M.J.L., Williams, O.R., Stewart, G.C., Saxton, R.D.,
 1992, MNRAS, 259, 743
 Ledlow, M.J., Owen, F.N., 1996, AJ, 112, 9
 Marchesini, D., Celotti, A., Ferrarese, L., 2004, MNRAS, 351, 733
 Müller, S.A.H., Haas, M., Siebenmorgen, R., Klaas, U., Meisenheimer, K.,
 Chini, R., Albrecht, M., 2004, A&A, 426, L29
 Ogle, P., Whysong, D., Antonucci, R., 2006, ApJ in press, astro-ph/0601485
 Pearson, T.J., 1996, in Hardee P.E., Bridle A.H., Zensus J.A., eds, Energy
 Transport in Radio Galaxies and Quasars, ASP Conference Series
 vol. 100, San Francisco, p. 97
 Piconcelli, E., Jimenez-Bailón, E., Guainazzi, M., Schartel, N., Rodríguez-
 Pascual, P.M., Santos-Lleó, M., 2005, A&A, 432, 15
 Rawlings, S., Saunders, R., 1991, Nat, 349, 138
 Rawlings, S., Saunders, R., Eales, S.A., Mackay, C.D., 1989, MNRAS, 240,
 701
 Reeves, J.N., Turner, M.J.L., 2000, MNRAS, 316, 234
 Reynolds, C.S., Brenneman, L.W., Stocke, J.T., 2005, MNRAS, 357, 381
 Reynolds, C.S., di Matteo, T., Fabian, A.C., Hwang, U., Canizares, C.R.,
 1996, MNRAS, 283, L111
 Sambruna, R.M., Eracleous, M., Mushotzky, R.F., 1999, ApJ, 526, 60
 Saunders, R., Baldwin, J.E., Rawlings, S., Warner, P.J., Miller, L., 1989,
 MNRAS, 238, 777
 Scheuer, P.A.G., 1987, in Zensus J., Pearson T., eds, Superluminal Radio
 Sources, Cambridge University Press, Cambridge, p. 104
 Smith, H.E., Spinrad, H., 1980, PASP, 92, 553
 Trussoni, E., Vagnetti, F., Massaglia, S., Feretti, L., Parama, P., Morganti,
 R., Fanti, R., Padovani, P., 1999, A&A, 348, 437
 Ueno, S., Koyama, K., Nishida, M., Yamauchi, S., Ward, M.J., 1994, ApJ,
 431, L1
 Urry, C.M., Padovani, P., 1995, PASP, 107, 803
 Varano, S., Chiaberge, M., Macchetto, F.D., Capetti, A., 2004, A&A, 428,
 401
 Willott, C.J., Rawlings, S., Blundell, K.M., Lacy, M., 1999, MNRAS, 309,
 1017
 Worrall, D.M., Birkinshaw, M., 1994, ApJ, 427, 134
 Worrall, D.M., Birkinshaw, M., 2005, MNRAS, 360, 926
 Worrall, D.M., Hardcastle, M.J., Pearson, T.J., Readhead, A.C.S., 2004,
 MNRAS, 347, 632
 Worrall, D.M., Lawrence, C.R., Pearson, T.J., Readhead, A.C.S., 1994, ApJ,
 420, L17

APPENDIX A: NOTES ON INDIVIDUAL SOURCES

A1 3C 28

The core of this low-excitation source is undetected in both radio and X-ray. We derive X-ray upper limits from the local count density, which is high as the source lies in the centre of one component of the merging cluster Abell 115 (e.g. Gutierrez & Krawczynski 2005). Limits on luminosities in absorbed and unabsorbed components were derived assuming photon indices of 1.7 and 2.0 respectively.

A2 3C 47

This quasar is reasonably well fitted ($\chi^2 = 62/48$) with a single power law model with $\Gamma = 1.5 \pm 0.1$, but when a second power law is added the fit is improved and the 90 per cent error on the normalization is non-zero, so we adopt that model. The single-power-law fit is consistent with earlier results (Lawson et al. 1992).

A3 3C 79

To our knowledge this is the first X-ray spectrum to be measured for this source. An unabsorbed and absorbed component are required by the data.

A4 3C 109

The moderate intrinsic absorption we find in the spectrum of this BLRG is in good agreement with the results of earlier *ROSAT* and *ASCA* observations (Allen & Fabian 1992; Allen et al. 1997) given the slightly different Galactic absorption column we adopt. The photon indices and spectral normalizations are also consistent within the joint 90 per cent confidence limits. We find no evidence for the iron line reported by Allen et al. (1997), although the signal to noise is relatively low in the *Chandra* data because of the annular extraction region we use.

A5 3C 123

The Galactic column density used for this source is taken from the earlier analysis of the *Chandra* data by Hardcastle et al. (2001) and the dominant (absorbed) power law model has similar parameters to the one fitted there. The large amount of Galactic reddening (the source is known to lie behind a molecular cloud) makes its classification as a low-excitation object uncertain. Chiaberge et al. (2002) show that its position on their diagnostic plane (equivalent width of [OIII] vs. optical to radio core flux ratio) is more consistent with a classification as a NLRG, and this would be consistent with the observed luminous, heavily absorbed nuclear X-ray component.

A6 3C 173.1

The small number of counts in the core of this low-excitation object means that only the normalization of X-ray models is constrained. Accordingly, the upper limit on the normalization of an obscured model is derived assuming that such a model produces *all* the observed counts.

A7 3C 192

When this source was fitted with the standard two-component power-law model there were prominent residuals in the range 0.5–1.0 keV, suggesting the addition of a thermal component. We obtained good fits by adding a MEKAL model with fixed $kT = 0.5$ keV and 0.5 solar abundance. To our knowledge the X-ray spectrum of this source has not been discussed elsewhere.

A8 3C 200

This source was classed as a NLRG by Belsole et al. (2006), following LRL, but the high-quality spectra of Laing et al. (1994) show it to be a LERG, and we adopt that classification here. Our spectral fits are, unsurprisingly, consistent with those of the analysis of the same data by Belsole et al.

A9 3C 215

The photon index for the single-power-law fit to this quasar is consistent with that found with *ASCA* by Reeves & Turner (2000), but its luminosity in our measurements is nearly a factor 2 lower, probably indicating variability.

A10 3C 219

We see no evidence in the spectrum of this broad-line radio galaxy for the excess absorption fitted by Sambruna et al. (1999) to *ASCA* data for the source, but there is a good deal of spatially resolved X-ray structure seen in the *Chandra* data (Comastri et al. 2003) which may have confused their fits.

A11 3C 223

The *XMM-Newton* data we use here were analysed by Croston et al. (2004). They fitted a model consisting of an unabsorbed power law, plus an absorbed power law and iron line; however, they fixed the photon index of the second power-law at $\Gamma = 1.5$, which leads to differences in the best-fitting spectral parameters. An apparent discrepancy in the flux densities obtained by the two analyses can be attributed to changes to the *XMM* calibration files since the work of Croston et al.

A12 3C 249.1

Both *Chandra* and *XMM-Newton* data exist for this quasar: we use only the *XMM* data, since there are more counts and no pileup issues to contend with. The best-fitting model includes a second power law with moderate intrinsic absorption, and a narrow Gaussian with rest-frame energy $6.42_{-0.06}^{+0.03}$ keV. The parameters of the double-power-law model are very similar to those fitted by Piconcelli et al. (2005) to the same X-ray data.

A13 3C 284

The *XMM-Newton* data we use here were analysed by Croston et al. (2004). Their best-fitting model parameters are in reasonable agreement with ours, although they fixed the photon index at $\Gamma = 1.5$, rather than 1.7 as used in this work. Apparent discrepancies in the absorption column affecting the second power-law component and in the flux densities result from changes in the *XMM* calibration files, as for 3C 223.

A14 3C 285

Ours is the first X-ray spectrum to be measured for the nucleus of this source. A two-component model with absorbed and unabsorbed power laws and a strong Gaussian component with rest-frame energy 6.42 ± 0.05 keV are required, although the data are not good enough to constrain the photon indices of the power-law components.

A15 3C 295

The longer observation we use allows us to fit a more sophisticated model to the data than was possible for Harris et al. (2000): the two-component best-fitting model explains the inverted spectrum found by Harris et al. when fitting a single power law with Galactic absorption. The addition of a narrow Gaussian component with rest-frame energy $6.4_{-0.5}^{+0.1}$ keV gives a significant improvement to the fits.

A16 3C 303

The power-law index we fit to this BLRG is consistent with the results from two sets of archival *ASCA* data reported by Kataoka et al. (2003). The luminosity inferred from the flux reported by Kataoka et al. is a factor ~ 1.5 higher than we observe, which may imply variability.

A17 3C 346

3C 346 is the only source classed as an FRI in our new sample. Worrall & Birkinshaw (2005) fitted a model with a small amount of intrinsic absorption to the *Chandra* data we use, and accordingly found a slightly steeper photon index and higher unabsorbed 1-keV flux density.

A18 3C 351

The parameters of the best-fitting model are similar to those found in the analysis of the same data in Hardcastle et al. (2002), but the photon index of the soft power law is even steeper than found in that paper. The change is presumably a result of updated responses for the ACIS-S detector.

A19 3C 388

The fits to this source are consistent with those in E06.

A20 3C 401

The parameters we fit for this source are consistent within the errors with those found by Reynolds, Brenneman & Stocke (2005) in their analysis of the same *Chandra* data.

A21 3C 436

The X-ray spectrum of this NLRG has not previously been investigated. In addition to the standard two-power-law model, residuals around 5 keV are reduced with the addition of a narrow Gaussian with rest-frame energy $6.4_{-0.1}^{+0.2}$ keV.

A22 3C 438

Our luminosity and photon index for this radio galaxy are consistent with the analysis of the same data in Donato et al. (2004).